Atmospheric Environment 179 (2018) 40–48

Contents lists available at ScienceDirect

Atmospheric Environment

journal homepage: www.elsevier.com/locate/atmosenv

Temperature effects on multiphase reactions of organic molecular markers: A modeling study

Vikram Pratap[a], Ying Chen[a], Guangming Yao[b,**], Shunsuke Nakao[a,*]

[a] Department of Chemical and Biomolecular Engineering, Clarkson University, Potsdam, NY, 13699, USA
[b] Department of Mathematics, Clarkson University, Potsdam, NY, 13699, USA

GRAPHICAL ABSTRACT

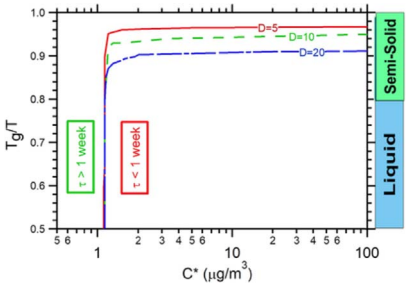

ARTICLE INFO

Keywords:
Markers
Levoglucosan
Biomass burning
Winter
Low-temperature
Saturation concentration
Diffusivity
Diffusion coefficient

ABSTRACT

Various molecular markers are used in source apportionment studies. In early studies, molecular markers were assumed to be inert. However, recent studies suggest that molecular markers can decay rapidly through multiphase reactions, which makes interpretation of marker measurements challenging. This study presents a simplified model to account for the effects of temperature and relative humidity on the lifetime of molecular markers through a shift in gas-particle partitioning as well as a change in viscosity of the condensed phase. As a model case, this study examines the stability of levoglucosan, a key marker species of biomass burning, over a wide temperature range relevant to summertime and wintertime. Despite the importance of wood combustion for space heating in winter, the lifetime of levoglucosan in wintertime is not well understood. The model predicts that in low-temperature conditions, levoglucosan predominantly remains in the particle phase, and therefore its loss due to gas-phase oxidation reactions is significantly reduced. Furthermore, the movement of the levoglucosan from the bulk of the particle to the particle surface is reduced due to low diffusivity in the semi-solid state. The simplified model developed in this study reasonably reproduces upper and lower bounds of the lifetime of levoglucosan investigated in previous studies. The model results show that the levoglucosan depletion after seven days reduces significantly from ~98% at 25 °C to < 1% at 0 °C under dry conditions. The depletion of levoglucosan increases at higher relative humidities. However, at temperatures below 0 °C, levoglucosan appears to be a useful marker (lifetime > 1 week) even at 60% relative humidity irrespective of the assumed fragility parameter *D* that controls estimated diffusivity. The model shows that lifetime of an organic molecular marker strongly depends on assumed *D* especially when a semi-volatile marker is in semi-solid organic aerosol.

* Corresponding author. Department of Chemical and Biomolecular Engineering, Clarkson University, 8 Clarkson Ave, Potsdam, NY, 13699, USA.
** Corresponding author.
E-mail addresses: gyao@clarkson.edu (G. Yao), snakao@clarkson.edu (S. Nakao).

https://doi.org/10.1016/j.atmosenv.2018.02.009
Received 1 September 2017; Received in revised form 1 February 2018; Accepted 3 February 2018
Available online 06 February 2018

1. Introduction

Biomass burning is one of the major primary sources of natural and anthropogenic pollutants (Gorin et al., 2006; Krecl et al., 2008; Pandis et al., 2016; Saarikoski et al., 2008; Saffari et al., 2013; von Schneidemesser et al., 2015). While western nations use biomass (including wood) for space heating and recreational purposes, several Asian, African and South American countries use it as a major energy resource. In the United States and Europe, domestic wood combustion is an important source of space heating and a significant source of particulate matter in winter (Caseiro et al., 2009; Crilley et al., 2015; Fine et al., 2002; Krecl et al., 2008; Szidat et al., 2006; Wang et al., 2011a, 2011b). Even though wood burning has been classified as a carbon neutral energy source, burning wood releases hazardous organic chemicals and particles, thereby increasing the aerosol burden on the atmosphere (Bari et al., 2011, 2009; Kim et al., 2013; Kocbach Bolling et al., 2009; Naeher et al., 2007; Shen et al., 2011).

In winter, the higher probability of temperature inversions and weak sunlight to break the inversion reduces the dilution of pollutants (Seinfeld and Pandis, 2006), and hence, wood smoke presents a significant risk to human health (World Health Organization, 2015).

The first step to framing control policies for wood smoke emissions is to correctly assess the contribution of wood smoke to air pollution. Therefore, a reliable quantitative marker is required to accurately quantify the contribution of wood smoke to ambient air pollution. Although non-mineral potassium (K) has been widely used as a marker species of biomass burning, the presence of other major sources (e.g., cooking) and the wide variability among wood types limit the utility of K as a marker species of wood smoke (Schauer et al., 2001). In contrast, organic markers tend to be more source-specific, but not inert. Levoglucosan, a chemical generated by pyrolysis of cellulose and hemicellulose during the biomass burning process, has been widely considered a useful molecular marker of biomass burning smoke over the last few decades (Elias et al., 2001; Fraser and Lakshmanan, 2000; Schauer and Cass, 2000; Simoneit et al., 2000, 2004, 1999, Simoneit and Elias, 2001, 2000). However, recent work (Hennigan et al., 2010) has questioned the assumed inertness of levoglucosan. They studied summertime chemistry experimentally and reported a short lifetime, or e-folding time, of levoglucosan on the order of 1–2 days. A theoretical study (May et al., 2012) also discussed the lifetime of levoglucosan and reported similar lifetimes. These studies also concluded that levoglucosan is semi-volatile, and hence its gas-phase oxidation in addition to the condensed phase oxidation can lead to its short lifetime. The apparent short lifetime of levoglucosan implies that air pollution source apportionment studies using levoglucosan as one of the markers may underestimate the contributions from biomass burning since aged smoke may be depleted in levoglucosan. Hence, the applicability of levoglucosan may be questionable at least under temperature conditions relevant to summer prescribed/wildfires. However, in winter, wood smoke emissions from residential stoves are significant contributors to air pollution. Additionally, lifetime of biomass burning markers at low temperatures may have significant implications for geochemical studies using biomass burning markers in ice cores to estimate wildfire several hundred years ago (Kawamura et al., 2012). At colder temperatures, gas-particle partitioning and condensed phase reactions are likely to significantly differ from those in summer.

Previous work (May et al., 2012) developed a model to account for oxidation of semi-volatile markers in the gas-phase and on the particle surface assuming particles are well-mixed. The model showed that temperature can have a significant effect on the lifetime of marker species primarily through the shift in gas-particle partitioning. On the other hand, an increasing number of studies suggest that viscosity of organic aerosol increases as a result of decrease in temperature, and therefore the particle interior cannot be assumed as well-mixed (Rothfuss and Petters, 2017; Shiraiwa et al., 2017). For instance, Arangio et al. (2015) investigated evolution of biomass burning markers, levoglucosan and abietic acid, using Kinetic Multi-layer model of Gas-Particle interactions (KM-GAP) that treats explicitly all steps of mass transfer and chemical reactions of organic compounds partitioning between gas, particle surface, and particle bulk phase. Their model suggests that temperature and relative humidity have significant influences on the lifetime of molecular markers by changing the viscosity and diffusivity of materials in aerosol particles. However, Arangio et al. (2015) did not include gas-phase oxidation of marker species, and hence, the lifetime predicted in their study is considered an upper limit.

This study builds upon previous studies that suggest gas-particle partitioning and condensed phase diffusivity may control the lifetime of biomass burning marker species. We hypothesize that under high-temperature conditions, the well-mixed assumption used in May et al. (2012) is appropriate, and under low-temperature conditions, diffusivity within particles may control the lifetime of marker species as in Arangio et al. (2015). We aim at bridging the gap by developing a simple model based on coupled ordinary and partial differential equations that can account for gas-particle partitioning as well as phase state of the particle. The model reasonably reproduces upper and lower bounds of the lifetime of levoglucosan suggested in previous studies. In addition, the model shows the transition of the lifetime of levoglucosan between low and high-temperature conditions. Even though this study focuses on levoglucosan, in principle, the same approach is applicable to a variety of organic molecular markers.

2. Model development

A system of differential equations is proposed to quantify the concentration of the levoglucosan in the particle and gas phase. The model is then non-dimensionalized and solved numerically. Fig. 1 illustrates the different processes taking place in the system. The assumptions and initial conditions used in framing the problem are as follows. The particle and gas phase levoglucosan are in equilibrium and uniform across respective phases at time $t = 0$. The overall loss of the levoglucosan is driven by the gas-phase reaction, particle phase reaction (on the particle surface) between levoglucosan and OH radical, and the equilibrium between the particle and the gas-phase levoglucosan.

Additionally, as the temperature declines, a larger amount of the levoglucosan partitions to the particle phase at equilibrium. For example, more than 99% of the total levoglucosan is estimated to partition to the particle phase at 0 °C, while only 75% at 25 °C. Equation (1) shows the gas-particle partitioning of a marker:

$$\xi_i = \left(1 + \frac{C_i^*(T)}{C_{OA}}\right)^{-1}, \tag{1}$$

where ξ_i is the fraction of the marker that stays in the particle at equilibrium, C_{OA} is the mass concentration of organic aerosol (OA), C_i^* is the saturation concentration of species i in a mixture. C_i^* is related to the saturation concentration C_i^O of a pure species i via the activity coefficient (ζ): $C_i^* = \zeta C_i^O$ (Donahue et al., 2011). Donahue et al. (2011) modeled ζ based on the similarity between solute (marker species) and solvent (OA) in terms of O/C ratio. Assuming levoglucosan (O/C = 0.83) is mixed in fresh biomass burning OA with O/C ≈ 0.25, ζ is estimated to be approximately 3 (Donahue et al., 2011). For aged OA with a higher O/C, ζ is expected to be closer to 1. This work assumes $\zeta = 1$ for simplicity since saturation concentration (C_i^O) is typically a much greater source of uncertainty with it typically being 1-2 orders of magnitude (Barley and McFiggans, 2010). The saturation concentration C^* at any temperature can be estimated using the Clausius-Clapeyron equation based on the heat of vaporization and C^* value at a reference temperature (May et al., 2012).

As the time passes, the gas phase concentration depletes and drives the mass transfer of the levoglucosan from the particle surface governed by gas-particle equilibrium. The loss of the levoglucosan concentration on the particle surface leads to the diffusion of the levoglucosan from

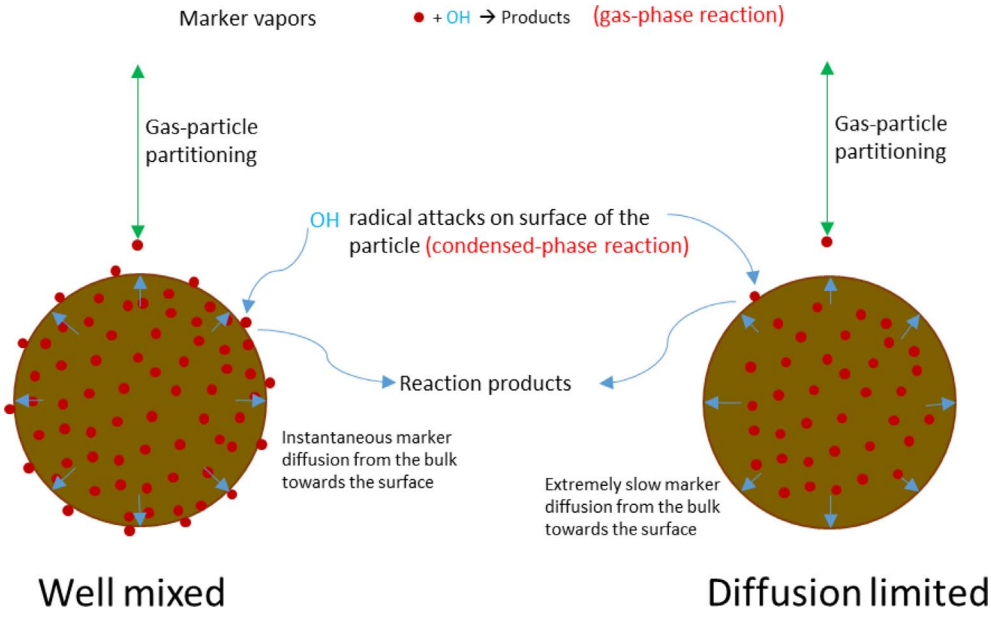

Fig. 1. A schematic of limiting cases considered in this study. The well-mixed case corresponds to high diffusivity within the condensed phase, while the diffusion limited case corresponds to low diffusivity. Diffusivity increases as temperature increases.

Table 1
Parameters and values at different conditions used in the hybrid model.

Parameter		Temperature (°C)			
		25	15	10	0
D_b (m^2/s)	Bulk diffusivity	1.41×10^{-20}	1.57×10^{-22}	1.19×10^{-23}	2.9×10^{-25}
d_p (nm)	Particle diameter	200	200	200	200
C^0_{lev} (μg/m^3)	Saturation concentration	13	3.157	1.498	0.311
D_g (m^2/s)	Gas phase diffusivity	5.00×10^{-6}	4.71×10^{-6}	4.57×10^{-6}	4.29×10^{-6}
F	Fucchs correction factor	0.4256	0.4403	0.4479	0.4635
N_t (#/cm^3)	Particle number concentration	8000	8000	8000	8000
K_e	Kelvin Effect	1.043	1.045	1.045	1.047
k_p (cm^3/molecule-s)	Particle-phase reaction rate constant	6.73×10^{-13}	6.84×10^{-13}	6.9×10^{-13}	7.01×10^{-13}
k_g (cm^3/molecule-s)	Gas-phase reaction rate constant	3.55×10^{-11}	3.47×10^{-11}	3.43×10^{-11}	3.34×10^{-11}
OH (molecule/cm^3)	Hydroxyl radical concentration	1.00×10^6	1.00×10^6	1.00×10^6	1.00×10^6
ρ (kg/m^3)	Particle density	1200	1200	1200	1200

*C_{OA} = 40 μg m^{-3}.

the particle bulk towards the surface. The phenomenon transforms to a radial concentration gradient across the particle which can be written as

$$\frac{\partial w_p(r,\,t)}{\partial t} = D_b\left(\frac{\partial^2 w_p(r,\,t)}{\partial r^2} + \frac{2}{r}\frac{\partial w_p(r,\,t)}{\partial r}\right),\ 0 < r \le R,\ t > 0, \tag{2}$$

On the other hand, the gas phase concentration of levoglucosan is

$$\frac{dC_g(t)}{dt} = 2\pi d_p D_g F N_t (w_p(R,\,t) K_e C^0_{lev} - C_g(t)) - k_g[OH]C_g(t), \tag{3}$$

And the initial and boundary conditions are the following:

$$w_p(r,\,0) = w_{p0} \tag{4.1}$$

$$C_g(0) = G_0 \tag{4.2}$$

$$\frac{\partial w_p(0,\,t)}{\partial r} = 0 \tag{4.3}$$

$$(\rho D_b \pi d_p^2 N_t)\frac{\partial w_p(R,\,t)}{\partial r} = -2\pi d_p D_g F N_t (w_p(R,\,t) K_e C^0_{lev} - C_g(t)) - k_p[OH] C_{OA} w_p(R,\,t) \tag{4.4}$$

where w_p (r, t) is the mass fraction of a marker species as a function of position r and time t, D_b is the bulk condensed phase diffusivity, R is the radius of a particle, C_g (t) is the gas-phase concentration of a marker species, d_p is the diameter of a particle ($d_p = 2R$), D_g is the gas-phase diffusivity of the marker, F is the Fuchs correction factor, N_t is the particle number concentration, K_e is the kelvin effect, C^0_{lev} is the saturation concentration of levoglucosan, k_g is the gas-phase reaction rate constant and [OH] is OH radical concentration, ρ is the density of the particle, w_{p0} and G_0 are the initial condensed phase fraction and gas-phase concentration respectively. $k_p = \gamma_{OH} J_{OH} MW_{OA}/C_{OA} N_A$ is the condensed phase reaction rate constant calculated using the collision theory method described in supplements of May et al. (2012). Briefly, γ_{OH} is OH radical uptake coefficient, J_{OH} is the collision frequency between OH radical and the particle, MW_{OA} is molecular weight of organic aerosol (OA), C_{OA} is OA concentration, and N_A is Avagadro's number. The term $w_p(R,\,t)K_e C^0_{lev}$ is the levoglucosan fraction on the surface of the particle for a diffusion limited case, and becomes $X_{m,lev} K_e C^0_{lev}$ when the condensed phase is well-mixed, where $X_{m,lev}$ is the mass fraction of levoglucosan in organic aerosol. Equation (4.3) accounts for symmetry of concentration profile at the particle center. Equation (4.4) is the flux boundary condition on the surface of the particle. The parameters and variables used in equations are described in Table 1.

Since the radius (nanometer) and time (days) scales are entirely

different, it would be difficult to find a convergent solution without non-dimensionalizing the variables, radius and time. After non-dimensionalizing radius and time, equations (2)–(4) can be re-written to yield Equations (5)–(7)

$$\frac{\partial w_p(x,\tau)}{\partial \tau} = \left(\frac{\partial^2 w_p(x,\tau)}{\partial x^2} + \frac{2}{x}\frac{\partial w_p(x,\tau)}{\partial x} \right), \quad 0 < x \le 1, \quad \tau > 0 \tag{5}$$

$$\frac{dC_g(\tau)}{d\tau} = \frac{R^2}{D_b}[2\pi d_p D_g F N_t (w_p(1,\tau) K_e C^0_{lev} - C_g(\tau)) - k_g [OH] C_g(\tau)]. \tag{6}$$

The initial and boundary conditions are

$$w_p(x,0) = w_{p0} \tag{7.1}$$

$$C_g(0) = G_0 \tag{7.2}$$

$$\frac{\partial w_p(0,\tau)}{\partial x} = 0 \tag{7.3}$$

$$\left(\frac{\rho D_b \pi d_p^2 N_t}{R}\right)\frac{\partial w_p(1,\tau)}{\partial x} = -2\pi d_p D_g F N_t (w_p(1,\tau) K_e C^0_{lev} - C_g(\tau)) - k_p [OH] C_{OA} w_p(1,\tau). \tag{7.4}$$

where x is the dimensionless parameter for radius, $x = r/R$, and τ is the dimensionless time, $\tau = D_b t/R^2$. Equations (5) and (6) are then solved numerically using the finite difference and Runge-Kutta methods. Further details of the model are discussed in the supplemental information. MATLAB codes that implement the algorithm are provided in the supplemental information.

The diffusivity of the organic aerosol within the condensed phase, D_b, is estimated using the technique described elsewhere (Angell, 1995; Derieux et al., 2017; Shiraiwa et al., 2017, 2011). The glass transition temperature T_g is calculated using the parameterization in terms of O/C of OA, proposed in Shiraiwa et al. (2017). Then the T_g-scaled Arrhenius plot of viscosity η vs. T_g/T is used to estimate the viscosity of the particle (Angell, 1995; Shiraiwa et al., 2017). The fragility parameter D determines the shape of η vs. T_g/T curve. The fragility parameter D provides the measure of the fragile behavior of the particle content. Lower D values indicate the particle is more fragile, which means the viscosity jump near T_g is relatively large compared to strong (non-fragile) particles. Additionally, at larger D values, viscosity follows Arrhenius plot, while at lower D values viscosity exhibits non-Arrhenius behavior with temperature. Fragility parameter D is assumed to be in the range of 5–20 for SOA, which is a low value range in overall D space. Higher D values results in a higher η (Shiraiwa et al., 2017). Using $D = 10$ as a base case (consistent with Shiraiwa et al. (2017)), viscosity is estimated and used to estimate the bulk diffusivity of the levoglucosan in the particle by applying Stokes-Einstein equation (Shiraiwa et al., 2011). The bulk diffusivity estimation discussed here is affected by relative humidity. Water acts as a plasticizer and significantly lowers viscosity (Koop et al., 2011), and hence enhances diffusivity, in the Stokes-Einstein relationship,

$$D_{org} = \frac{kT}{6\pi a \nu}, \tag{8}$$

where k is the Boltzmann constant, T is the temperature, a is the effective molecular radius (assumed to be 0.69 nm for levoglucosan (Shiraiwa et al., 2012)), and ν is the dynamic viscosity. Here, we perform a simple evaluation to illustrate potential impacts of water on the decay of molecular markers.

The calculation of viscosity in this study is based on T_g/T ratio as shown in Shiraiwa et al. (2017) (Fig. 2). T_g of the organic aerosol is calculated using the parameterization provided in Shiraiwa et al. (2017),

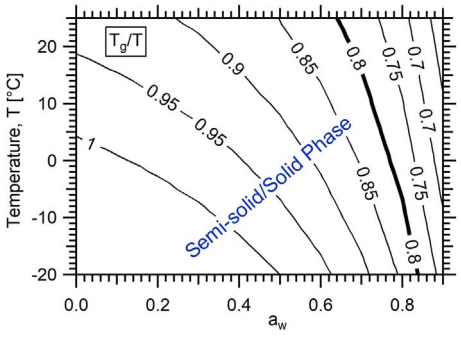

Fig. 2. Estimated effect of temperature and water activity on T_g/T using O/C = 0.8, $\kappa = 0.1$, $\rho_{org} = 1.2\,g\,cm^{-3}$. $T_g/T = 0.8$ is assumed to be the threshold between liquid and semi-solid state (Shiraiwa et al., 2017).

$$T_{g,i} = A + BM + CM^2 + D\left(\frac{O}{C}\right) + EM\left(\frac{O}{C}\right), \tag{9}$$

where M is the molar mass (g mol^{-1}), O/C is the oxygen-to-carbon ratio of organics, and A, B, C, D, and E are empirically determined coefficients. Average values of coefficients are $A = -21.57$ K, $B = 1.51$ K mol g^{-1}, $C = -1.7 \times 10^{-3}$ K mol^2 g^{-2}, $D = 131.4$ K, and $E = -0.25$ K mol g^{-1}. For instance, assuming $M = 250$ g mol^{-1}, O/C ratio of the organic aerosol 0.4, $T_{g,OA}$ is estimated to be 4 °C.

The Gordon-Taylor mixing rule is used to estimate T_g of organics mixed with water:

$$T_g(w_{org}) = \frac{(1 - w_{org})T_{g,w} + \frac{1}{k_{GT}} w_{org} T_{g,org}}{(1 - w_{org}) + \frac{1}{k_{GT}} w_{org}}, \tag{10}$$

where w_{org} is the mass fraction of organics, $T_{g,w}$ is the glass transition temperature of pure water (136 K), and k_{GT} is the Gordon-Taylor constant, assumed to be 2.5 ± 1.0 (Shiraiwa et al., 2017). Although k_{GT} is highly uncertain, equation (10) allows simple evaluation of the effects of relative humidity (RH) on T_g. Assuming a particle is comprised of organics only, w_{org} can be calculated using the single hygroscopicity parameter, κ (Petters and Kreidenweis, 2007):

$$w_{org} = \left(1 + \frac{\kappa \rho_w}{\rho_{org}} \frac{a_w}{1 - a_w}\right)^{-1}, \tag{11}$$

where ρ_w is the density of pure water, ρ_{org} is the density of organics, and a_w is the activity of water which is equivalent to RH for a flat surface. We assumed $\kappa = 0.1$, $\rho_w = 1\,g\,cm^{-3}$, and $\rho_{org} = 1.2\,g\,cm^{-3}$. Using these values, T_g/T can be estimated for a combination of T and RH (or a_w) as shown in Fig. 2. $T_g/T = 0.8$ is assumed to be an approximate threshold between the liquid state and semi-solid state. Any combination of T and a_w following a contour line would result in the same viscosity in our simplified model framework. For instance, the system at 4 °C in dry conditions ($a_w = 0$) is equivalent to a system at −20 °C and $a_w = 0.5$, represented by $T_g/T = 1$ curve. Although temperature is a part of the Stokes-Einstein equation (Equation (8)), its major impact is through changes in viscosity spanning many orders of magnitude. Therefore, all the model calculations for dry conditions shown in this study can be approximately translated into different RH conditions following the contour lines of T_g/T in Fig. 2.

In summary, our model discussed above builds upon the model from May et al. (2012) by accounting for diffusion limitations that may result in the particles being not well-mixed, thereby extending the applicability of the model to any aerosol phase (liquid, semi-solid, or solid). This model addresses some of the questions explored in Arangio et al. (2015), such as lifetime of levoglucosan in a semi-solid paricle, while accounting for gas-phase chemistry using a relatively simple set of coupled differential equations.

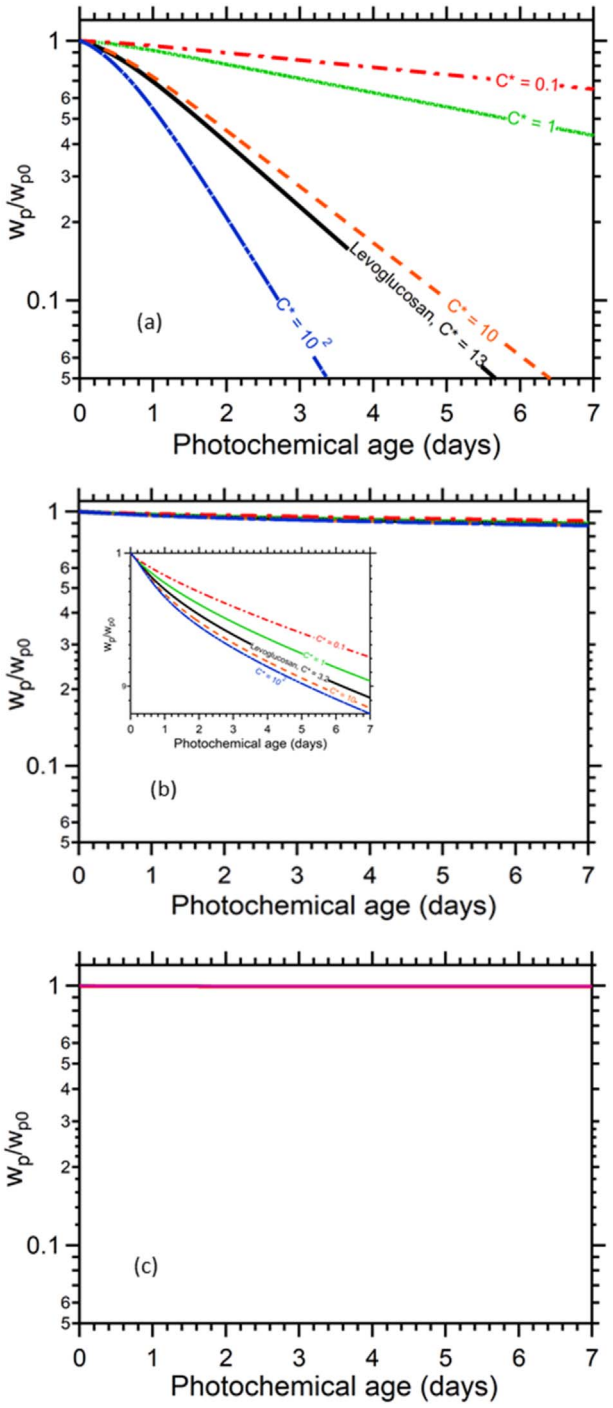

Fig. 3. Aging of levoglucosan and other molecular markers at different temperatures (a) 25 °C, (b) 15 °C and (c) 0 °C using the fragility parameter $D = 10$.

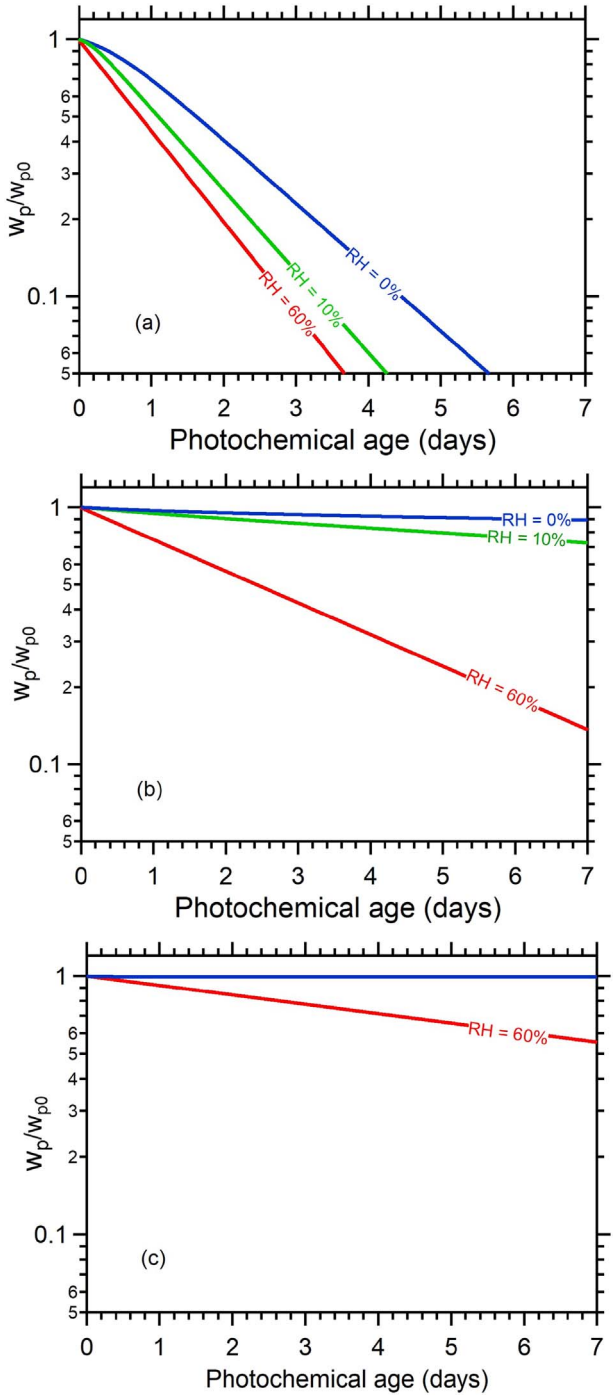

Fig. 4. The decay of levoglucosan at different humidities and different temperatures (a) 25 °C, (b) 15 °C and (c) 0 °C using the fragility parameter $D = 10$.

3. Results and discussions

Fig. 3 shows the levoglucosan concentration in the particle phase integrated over the entire volume at each time for different temperatures at 0% relative humidity and fragility parameter $D = 10$. For comparison, Fig. 3 includes model simulations of hypothetical compounds with different saturation concentrations ($C^* = 0.1$, 1, 10, 100 μg/m^3) assuming the molecular weight of levoglucosan (162 g/mol). It can be seen in Fig. 3 that the degradation of an organic marker significantly slows down below 15 °C. At warmer temperatures (25 °C), levoglucosan lifetime (e-folding time) is just two days. Even at warm temperatures (Fig. 3(a)), compounds with vapor pressures ≤ 1 μg/m^3 appear to be useful marker. Fig. 3(b) shows that the temporal evolution dramatically slowed down at 15 °C. Fig. 4, on the other hand, illustrates the impact of water on the oxidation of levoglucosan at different temperatures and humidities. Levoglucosan depletes faster as the relative humidity increases from 0% to 60% at all temperatures. Fig. 4(b) shows that depletion of levoglucosan is most sentive to relative humidity at 15 °C. This is because at high/low temperature, the viscosity (or diffusivity) is sufficiently low/high irrespective of relative humidity. Overall, levoglucosan appears to be a useful marker at temperatures below 0 °C even at high humidity. If organics are internally mixed with inorganics, the effects of RH should be even more pronounced. Thus, further studies on the effects of mixing states and hygroscopicity on the

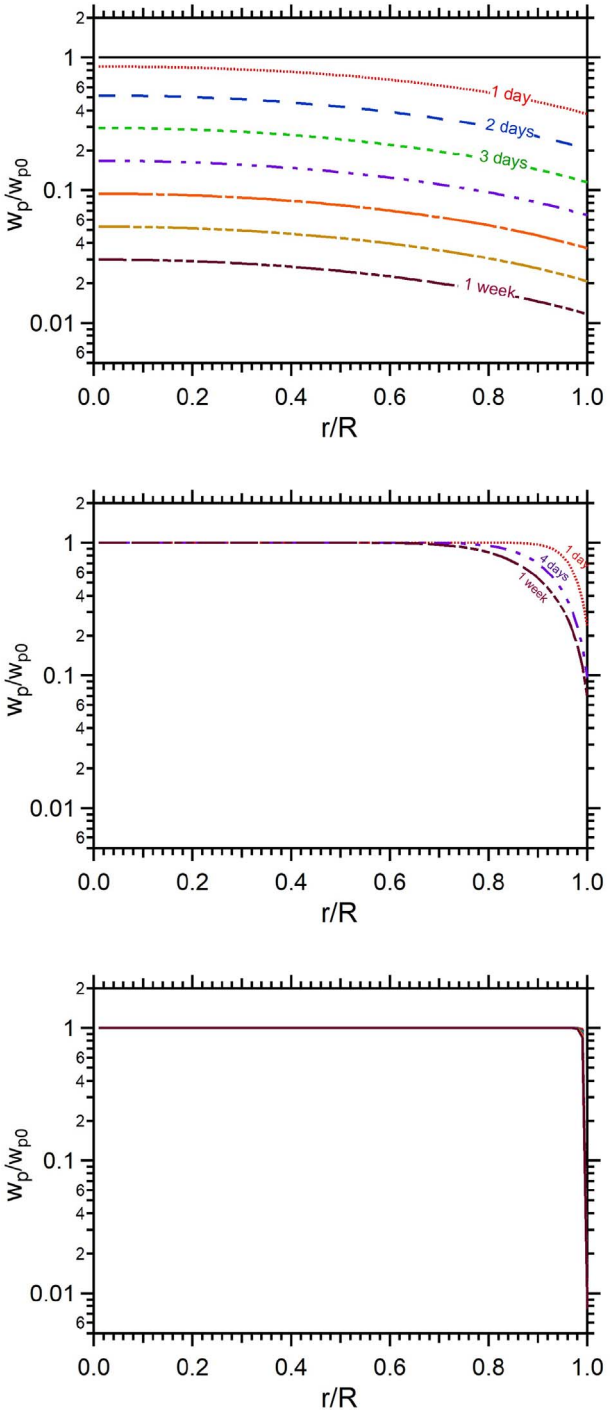

Fig. 5. Concentration profiles inside the particle at different temperatures (a) 25 °C, (b) 15 °C and (c) 0 °C cases. Fragility parameter $D = 10$ is used.

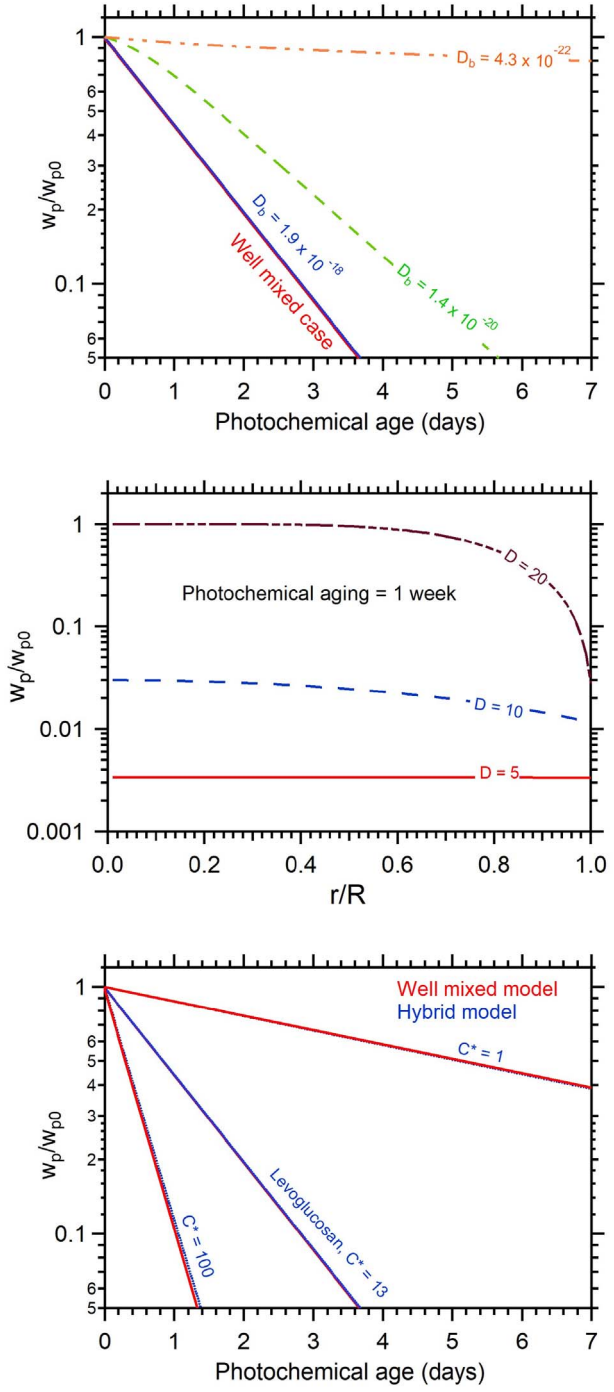

Fig. 6. Variation in the total concentration and concentration profile at 25 °C. (a) compares the hybrid model with the well-mixed May et al. model of levoglucosan at different diffusivities corresponding to the values of fragility parameter $D = 5$, 10, and 20, (b) observes the effect of fragility parameter D on the time evolution of levoglucosan after one week of photochemical aging assuming OH = 10^6 molecule cm^{-3}, and (c) compares the applicability of this model for other hypothetical compounds of different saturation concentration with well-mixed model using the $D_b = 1.9 \times 10^{-18}$ m^2/s.

lifetime of molecular marker species will be beneficial.

In order to assess the role of diffusivity within the condensed phase, Fig. 5 shows the radial distribution of levoglucosan within a particle at different temperatures. At 15 °C, 60% of the particle core remains intact, and at 0 °C, 98% of the particle core concentration does not change significantly after 1 week. This suggests that bulk diffusivity of the compound plays a critical role in the loss of a compound. At higher temperatures, high diffusivity leads to faster evaporation and more significant gas-phase oxidation, and at low temperatures, low diffusivity preserves the compound.

To test the model, the model results for levoglucosan were compared with the well-mixed model of May et al. (2012) as a base case in Fig. 6(a). The levoglucosan concentration curve matches well with the well-mixed model at the bulk diffusivity 1.9×10^{-18} m^2/s estimated using the fragility parameter $D = 5$. The bulk diffusivity of 10^{-18} is approximately the lowest limit at which this model matches well with the well-mixed case. Calculating the characteristic time of diffusion as $\tau_D = R^2/(\pi^2 D_{org})$ (Shiraiwa et al., 2011) assuming a 100 nm particle, the bulk diffusivity corresponds to a characteristic time of a few minutes, consistent with the well-mixed behavior. At other diffusivities

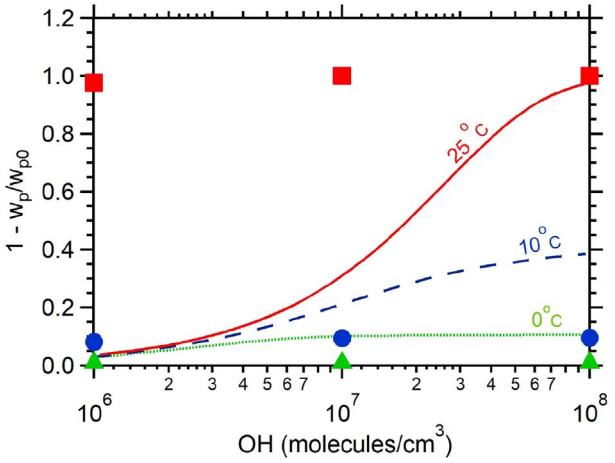

Fig. 7. Model comparison between this study and Arangio et al. (2015) at different temperatures. *y*-axis is the amount of the levoglucosan lost after 1 week of reaction with OH at different concentrations. The lines represent Arangio et al. (2015) while the symbols are from this work at corresponding temperatures.

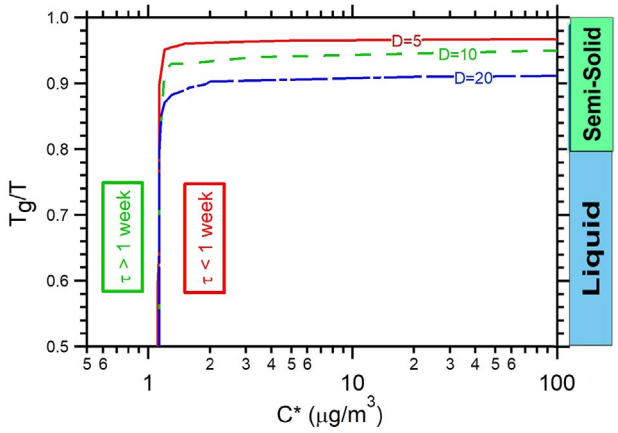

Fig. 8. Thresholds for 1 week lifetime of hypothetical compounds at different fragility parameter *D*. Region below each plot corresponds to the unstable zone (lifetimetime < 1 week) and vice versa.

1.4×10^{-20} m^2/s and 4.3×10^{-22} m^2/s, corresponding to $D = 10$ and 20 respectively, the characteristic times are 5 h and 7 days respectively, leading to a significant disagreement with the well-mixed case (May et al., 2012). This disagreement is evident in Fig. 6(b). The concentration profile inside the particle in Fig. 6(b) shows that at a fragility parameter of $D = 5$, there is no significant concentration gradient within the particle implying the well-mixed state. However, for other *D* values, the concentration changes radially, and therefore the particle-phase is not well-mixed. It can be seen in Fig. 6(c) that our model agrees well with the well-mixed model over a wide range of hypothetical chemicals with different volatilities.

Fig. 7 compares the levoglucosan degradation fraction after one week of aging at different temperatures and [OH] radical concentration with the results of Arangio et al. (2015). The fraction estimated from our model agrees reasonably well at low temperatures and atmospherically relevant [OH] concentrations ~ 10^6 molecule cm^{-3}, but deviate significantly at 25 °C. This difference is possibly due to the non-inclusion of gas-phase chemistry in the KM-GAP model. At higher [OH] concentrations, no noticeable variation is observed in the levoglucosan concentration in our model, unlike Arangio et al. (2015). Although the reason for the discrepancy is unclear, the different treatment of condensed phase OH oxidation between this study and Arangio et al. (2015) may partly explain the discrepancy. This study assumes OH oxidation occurs in the gas-phase (Equation (6)) and on the particle surface (Equation (7.4)) only. Arangio et al. (2015) considers diffusion of OH into the near-surface bulk. They showed an example case at OH = 5×10^{10} molecules cm^{-3} with ~1 nm diffusion of OH from the particle surface. Since the concentration gradient of levoglucosan is very steep near the particle surface at lower temperatures, OH would encounter higher mass fraction of levoglucosan in the near-surface bulk than on the surface layer. Therefore, our simplified model may underestimate condensed phase reaction, which may lead to underestimation of levoglucosan loss at high OH concentration when the gas-phase is depleted of levoglucosan. However, we emphasize that under a typical OH concentration of ~10^6 molecules cm^{-3}, our model successfully shows a substantial increase in lifetime due to diffusion limitation at low temperatures (Figs. 5 and 7), as well as rapid decay via gas-phase reaction within one model framework.

Even though our model assumed 1×10^6 molecules/cm^3 OH concentration (except for Fig. 7), atmospheric OH concentration is generally assumed to be low in winter due to lower absolute humidity and ozone as well as weaker/shorter sunlight. The lower OH concentration will have direct effects on the lifetime of levoglucosan. For instance, at OH = 0.1×10^6 molecule/cm^3, the estimated lifetime of levoglucosan should increase by ten-fold. In polluted regions, however, OH concentrations in winter may be comparable to that in summer due to photolysis of HONO (Huang et al., 2014) or aldehydes (Edwards, 2014). A recent study (Huang et al., 2014) used Geos-Chem model to estimate OH concentration in northern China during the winter haze event in 2013 and predicted OH concentrations of at least 0.4×10^6 molecules/cm^3.

Fig. 8 illustrates the sensitivity of a lifetime of 7 days on the saturation concentration and T_g/T ratio at different fragility parameter. Shiraiwa et al. suggest that $T_g/T = 0.8$ corresponds to liquid/semi-solid threshold and $T_g/T = 1.0$ corresponds to semi-solid/solid threshold. The simulation assumes a temperature range of 273–298 K. Fig. 8 shows that when 1-week lifetime is taken as a threshold for reasonably stable marker species, the fragility parameter does not appear to shift the threshold when $T_g/T < 0.8$, consistent with a well-mixed liquid state. In case of a liquid particle, the lifetime is dictated by C^* as shown in May et al. (2012). At T_g/T around 0.9–1.0, variability in *D* can significantly change the lifetime. At $T_g/T > 1.0$, viscosity is so low that a marker molecule would be effectively stable irrespective of *D* and volatility (C*). Therefore, the uncertainty in *D* is particularly important for a marker species with C* > 1–2 μg/m^3 in semi-solid OA. The model also suggests that organic markers with saturation concentration ≤1 μg/m^3 are practically stable irrespective of diffusivity.

The model neglects other factors such as particle size-distribution, reactions with other oxidants such as NO_3 (Shiraiwa et al., 2012), and photosensitized reactions (George et al., 2015). The estimate of diffusivity based on O/C parameterization of T_g is still exploratory and needs further verifications. Therefore, the simplified model presented in this study should be taken as a guide to identify the conditions where the well-mixed assumption used for calculation of marker species in May et al. (2012) is violated while maintaining the mathematical simplicity of coupled differential equations. Potential applications of this study includes low temperature photochemistry of molecular markers in free troposphere during long-range transport of organic aerosols. Previous studies found that the particle physical state remains as semi-solid/solid state in free troposphere region (Rothfuss and Petters, 2017). Improved understanding of the stability of markers in free troposphere may provide additional insights on particle source-apportionment studies.

4. Conclusions

This work presents a simple model for predicting the lifetime of a marker species with respect to oxidation by OH in the atmosphere. The model considers OH oxidation in the gas-phase and on the particle surface as well as mass transfer within the condensed phase. Even though it is a simplified model, the model reasonably reproduces the

upper and lower bounds of the marker lifetime predicted by the well-mixed and KM-GAP model at OH ≈ 10^6 molecule cm^{-3} under a wide temperature range. The bulk-phase diffusivity of 10^{-18} m^2/s is perhaps the lower limit of the diffusivity to treat an organic aerosol as well-mixed. The atmospheric lifetime of chemicals with the saturation concentration ≤1 μg/m^3 is estimated to be generally over one week even at warm and humid conditions. The model suggests that the lifetime of markers increases significantly below 15 °C based on an estimated viscosity using fragility parameter $D = 10$, although the value of D is still highly uncertain. Under dry conditions with $D = 10$, approximately 98% of levoglucosan is depleted at 25 °C whereas ≤1% is lost at 0 °C after seven days of aging. Despite the uncertainty in D, the lifetime of levoglcucosan below 0 °C is generally over one week even at higher humidities (60%). The apparent long lifetime of levoglucosan in winter temperature indicates that levoglucosan can be a useful marker for winter conditions. The model extends the work by May et al. (2012) by relaxing the well-mixed assumption in the condensed phase. The model shows the transition from the well-mixed case into diffusion limited case as viscosity increases, approaching the condition studied by Arangio et al. (2015) within one framework. This work highlights the coupled effect of volatility and viscosity in winter conditions. Further work is necessary, especially in validating the effects of water on marker lifetime.

Author contributions

V.P. created the well-mixed model using Igor Pro, worked on the PDE model and performed calculations in different scenarios, and wrote this publication, S.N. conceived the model framework and reviewed the publication, Y.C. created a preliminary MATLAB code for solving the system of PDEs, G.Y. supervised Y.C. and V.P. in MATLAB code and numerical methods development and reviewed the publication.

Conflicts of interest

"The authors declare no conflict of interest".

Acknowledgements

We acknowledge funding support from the New York State Energy Research and Development Authority (NYSERDA), agreement number 59809, and the Department of Chemical and Biomolecular Engineering, Clarkson University. We also thank Prof. Philip K. Hopke and Dr. Ellen G. Burkhard for helpful discussions.

Appendix A. Supplementary data

The details of the model are discussed in the form of a pdf file and the MATLAB partial differential equation (PDE) model code.

Supplementary data related to this article can be found at http://dx.doi.org/10.1016/j.atmosenv.2018.02.009.

References

Angell, C.A., 1995. Formation of glasses from liquids and biopolymers. Science 267, 1924–1935. http://dx.doi.org/10.1126/science.267.5206.1924.

Arangio, A.M., Slade, J.H., Berkemeier, T., Pöschl, U., Knopf, D. a., Shiraiwa, M., 2015. Multiphase chemical kinetics of OH radical uptake by molecular organic markers of biomass burning aerosols: humidity and temperature dependence, surface reaction, and bulk diffusion. J. Phys. Chem. A. http://dx.doi.org/10.1021/jp510489z. 150225115449002.

Bari, M.A., Baumbach, G., Brodbeck, J., Struschka, M., Kuch, B., Dreher, W., Scheffknecht, G., 2011. Characterisation of particulates and carcinogenic polycyclic aromatic hydrocarbons in wintertime wood-fired heating in residential areas. Atmos. Environ. 45, 7627–7634. https://doi.org/10.1016/j.atmosenv.2010.11.053.

Bari, M.A., Baumbach, G., Kuch, B., Scheffknecht, G., 2009. Wood smoke as a source of particle-phase organic compounds in residential areas. Atmos. Environ. 43, 4722–4732. http://dx.doi.org/10.1016/j.atmosenv.2008.09.006.

Barley, M.H., McFiggans, G., 2010. The critical assessment of vapour pressure estimation methods for use in modelling the formation of atmospheric organic aerosol. Atmos. Chem. Phys. 10, 749–767. http://dx.doi.org/10.5194/acp-10-749-2010.

Caseiro, A., Bauer, H., Schmidl, C., Pio, C.A., Puxbaum, H., 2009. Wood burning impact on PM10 in three Austrian regions. Atmos. Environ. 43, 2186–2195. https://doi.org/10.1016/j.atmosenv.2009.01.012.

Crilley, L.R., Bloss, W.J., Yin, J., Beddows, D.C.S., Harrison, R.M., Allan, J.D., Young, D.E., Flynn, M., Williams, P., Zotter, P., Prevot, A.S.H., Heal, M.R., Barlow, J.F., Halios, C.H., Lee, J.D., Szidat, S., Mohr, C., 2015. Sources and contributions of wood smoke during winter in London: assessing local and regional influences. Atmos. Chem. Phys. 15, 3149–3171. http://dx.doi.org/10.5194/acp-15-3149-2015.

Derieux, W.W., Li, Y., Lin, P., Laskin, J., Laskin, A., 2017. Predicting the Glass Transition Temperature and Viscosity of Secondary Organic Material Using Molecular Composition. pp. 1–41.

Donahue, N.M., Epstein, S. a., Pandis, S.N., Robinson, a. L., 2011. A two-dimensional volatility basis set: 1. organic-aerosol mixing thermodynamics. Atmos. Chem. Phys. 11, 3303–3318. http://dx.doi.org/10.5194/acp-11-3303-2011.

Elias, V.O., Simoneit, B.R.T., Cordeiro, R.C., Turcq, B., 2001. Evaluating levoglucosan as an indicator of biomass burning in Carajás, amazônia: a comparison to the charcoal record. Geochim. Cosmochim. Acta 65, 267–272. http://dx.doi.org/10.1016/S0016-7037(00)00522-6.

Fine, P.M., Cass, G.R., Simoneit, B.R.T., 2002. Chemical characterization of fine particle emissions from the fireplace combustion of woods grown in the Southern United States. Environ. Sci. Technol. 36, 1442–1451. http://dx.doi.org/10.1021/es0108988.

Fraser, M.P., Lakshmanan, K., 2000. Using levoglucosan as a molecular marker for the long-range transport of biomass combustion aerosols. Environ. Sci. Technol. 34, 4560–4564. http://dx.doi.org/10.1021/es991229l.

George, C., Ammann, M., D'Anna, B., Donaldson, D.J., Nizkorodov, S.A., 2015. Heterogeneous photochemistry in the atmosphere. Chem. Rev. http://dx.doi.org/10.1021/cr500648z.

Gorin, C.A., Collett, J.L., Herckes, P., 2006. Wood smoke contribution to winter aerosol in fresno, CA. J. Air Waste Manage. Assoc 56, 1584–1590. http://dx.doi.org/10.1080/10473289.2006.10464558.

Hennigan, C.J., Sullivan, A.P., Collett, J.L., Robinson, A.L., 2010. Levoglucosan stability in biomass burning particles exposed to hydroxyl radicals. Geophys. Res. Lett. 37, L09806. http://dx.doi.org/10.1029/2010GL043088.

Huang, R.J., Zhang, Y., Bozzetti, C., Ho, K.F., Cao, J.J., Han, Y., Daellenbach, K.R., Slowik, J.G., Platt, S.M., Canonaco, F., Zotter, P., Wolf, R., Pieber, S.M., Bruns, E.A., Crippa, M., Ciarelli, G., Piazzalunga, A., Schwikowski, M., Abbaszade, G., Schnelle-Kreis, J., Zimmermann, R., An, Z., Szidat, S., Baltensperger, U., El Haddad, I., Prevot, A.S., 2014. High secondary aerosol contribution to particulate pollution during haze events in China. Nature 514, 218–222. http://dx.doi.org/10.1038/nature13774.

Kawamura, K., Izawa, Y., Mochida, M., Shiraiwa, T., 2012. Ice core records of biomass burning tracers (levoglucosan and dehydroabietic, vanillic and p-hydroxybenzoic acids) and total organic carbon for past 300years in the Kamchatka Peninsula, Northeast Asia. Geochim. Cosmochim. Acta 99, 317–329. http://dx.doi.org/10.1016/j.gca.2012.08.006.

Kim, K.-H., Jahan, S.A., Kabir, E., Brown, R.J.C., 2013. A review of airborne polycyclic aromatic hydrocarbons (PAHs) and their human health effects. Environ. Int. 60, 71–80. https://doi.org/10.1016/j.envint.2013.07.019.

Kocbach Bolling, A., Pagels, J., Yttri, K., Barregard, L., Sallsten, G., Schwarze, P., Boman, C., 2009. Health effects of residential wood smoke particles: the importance of combustion conditions and physicochemical particle properties. Part. Fibre Toxicol. 6, 29.

Koop, T., Bookhold, J., Shiraiwa, M., Pöschl, U., 2011. Glass transition and phase state of organic compounds: dependency on molecular properties and implications for secondary organic aerosols in the atmosphere. Phys. Chem. Chem. Phys. 13, 19238. http://dx.doi.org/10.1039/c1cp22617g.

Krecl, P., Hedberg Larsson, E., Ström, J., Johansson, C., 2008. Contribution of residential wood combustion and other sources to hourly winter aerosol in Northern Sweden determined by positive matrix factorization. Atmos. Chem. Phys. 8, 3639–3653. http://dx.doi.org/10.5194/acp-8-3639-2008.

May, A.A., Saleh, R., Hennigan, C.J., Donahue, N.M., Robinson, A.L., 2012. Volatility of organic molecular markers used for source apportionment analysis: measurements and implications for atmospheric lifetime. Environ. Sci. Technol. 46, 12435–12444. http://dx.doi.org/10.1021/es302276t.

Naeher, L.P., Brauer, M., Lipsett, M., Zelikoff, J.T., Simpson, C.D., Koenig, J.Q., Smith, K.R., 2007. Woodsmoke health effects: a review. Inhal. Toxicol. 19, 67–106. http://dx.doi.org/10.1080/08958370600985875.

Pandis, S.N., Skyllakou, K., Florou, K., Kostenidou, E., Kaltsonoudis, C., Hasa, E., Presto, A.A., 2016. Urban particulate matter pollution: a tale of five cities. Faraday Discuss 189, 277–290. http://dx.doi.org/10.1039/C5FD00212E.

Petters, M.D., Kreidenweis, S.M., 2007. A single parameter representation of hygroscopic growth and cloud condensation nucleus activity. Atmos. Chem. Phys. 1961–1971.

Rothfuss, N.E., Petters, M.D., 2017. Characterization of the temperature and humidity-dependent phase diagram of amorphous nanoscale organic aerosols. Phys. Chem. Chem. Phys. 19, 6532–6545. http://dx.doi.org/10.1039/C6CP08593H.

Saarikoski, S., Sillanpää, M., Saarnio, K., Hillamo, R., Pennanen, A., Salonen, R., 2008. Impact of biomass combustion on urban fine particulate matter in Central and Northern Europe. Water. Air. Soil Pollut 191, 265–277. http://dx.doi.org/10.1007/s11270-008-9623-1.

Saffari, A., Daher, N., Samara, C., Voutsa, D., Kouras, A., Manoli, E., Karagkiozidou, O., Vlachokostas, C., Moussiopoulos, N., Shafer, M.M., Schauer, J.J., Sioutas, C., 2013. Increased biomass burning due to the economic crisis in Greece and its adverse impact on wintertime air quality in Thessaloniki. Environ. Sci. Technol. 47, 13313–13320. http://dx.doi.org/10.1021/es403847h.

Schauer, J.J., Cass, G.R., 2000. Source apportionment of wintertime gas-phase and

particle-phase air pollutants using organic compounds as tracers source apportionment of wintertime gas-phase and particle-phase air pollutants using organic compounds as tracers. Environ. Sci. Technol. 34, 1821–1832. http://dx.doi.org/10.1021/es981312t.

Schauer, J.J., Kleeman, M.J., Cass, G.R., Simoneit, B.R.T., 2001. Measurement of emissions from air pollution sources. 3. C1 − C29 organic compounds from fireplace combustion of wood. Environ. Sci. Technol. 35, 1716–1728. http://dx.doi.org/10.1021/es001331e.

Seinfeld, J.H., Pandis, S.N., 2006. Atmospheric chemistry and physics: from air pollution to climate change. Atmos. Chem. Phys. http://dx.doi.org/10.1063/1.882420.

Shen, G., Tao, S., Wang, W., Yang, Y., Ding, J., Xue, M., Min, Y., Zhu, C., Shen, H., Li, W., Wang, B., Wang, R., Wang, W., Wang, X., Russell, A.G., 2011. Emission of oxygenated polycyclic aromatic hydrocarbons from indoor solid fuel combustion. Environ. Sci. Technol. 45, 3459–3465. http://dx.doi.org/10.1021/es104364t.

Shiraiwa, M., Ammann, M., Koop, T., Pöschl, U., 2011. Gas uptake and chemical aging of semisolid organic aerosol particles. Proc. Natl. Acad. Sci. U. S. A 108, 11003–11008. http://dx.doi.org/10.1073/pnas.1103045108.

Shiraiwa, M., Li, Y., Tsimpidi, A.P., Karydis, V.A., Berkemeier, T., Pandis, S.N., Lelieveld, J., Koop, T., Pöschl, U., 2017. Global distribution of particle phase state in atmospheric secondary organic aerosols. Nat. Commun. 8, 15002. http://dx.doi.org/10.1038/ncomms15002.

Shiraiwa, M., Pöschl, U., Knopf, D.A., 2012. Multiphase chemical kinetics of NO3 radicals reacting with organic aerosol components from biomass burning. Environ. Sci. Technol. 46, 6630–6636. http://dx.doi.org/10.1021/es300677a.

Simoneit, B.R., Elias, V., 2001. Detecting organic tracers from biomass burning in the atmosphere. Mar. Pollut. Bull. 42, 805–810. http://dx.doi.org/10.1016/S0025-326X(01)00094-7.

Simoneit, B.R., Oros, D., Elias, V., 2000. Molecular tracers for smoke from charring/burning of chitin biopolymer. Chemosph. - Glob. Chang. Sci 2, 101–105. http://dx.doi.org/10.1016/S1465-9972(99)00049-5.

Simoneit, B.R.T., Elias, V.O., 2000. Organic tracers from biomass burning in atmospheric particulate matter over the ocean. Mar. Chem. 69, 301–312. http://dx.doi.org/10.1016/S0304-4203(00)00008-6.

Simoneit, B.R.T., Elias, V.O., Kobayashi, M., Kawamura, K., Rushdi, A.I., Medeiros, P.M., Rogge, W.F., Didyk, B.M., 2004. Sugars–dominant water-soluble organic compounds in soils and characterization as tracers in atmospheric particulate matter. Environ. Sci. Technol. 38, 5939–5949. http://dx.doi.org/10.1021/es0403099.

Simoneit, B.R.T., Schauer, J.J., Nolte, C.G., Oros, D.R., Elias, V.O., Fraser, M.P., Rogge, W.F., Cass, G.R., 1999. Levoglucosan, a tracer for cellulose in biomass burning and atmospheric particles. Atmos. Environ. 33, 173–182. http://dx.doi.org/10.1016/S1352-2310(98)00145-9.

Szidat, S., Jenk, T.M., Synal, H.-A., Kalberer, M., Wacker, L., Hajdas, I., Kasper-Giebl, A., Baltensperger, U., 2006. Contributions of fossil fuel, biomass-burning, and biogenic emissions to carbonaceous aerosols in Zurich as traced by 14C. J. Geophys. Res. Atmos. 111http://dx.doi.org/10.1029/2005JD006590. n/a-n/a.

von Schneidemesser, E., Monks, P.S., Allan, J.D., Bruhwiler, L., Forster, P., Fowler, D., Lauer, A., Morgan, W.T., Paasonen, P., Righi, M., Sindelarova, K., Sutton, M. a, 2015. Chemistry and the linkages between air quality and climate change. Chem. Rev. http://dx.doi.org/10.1021/acs.chemrev.5b00089. 150430065937004.

Wang, Y., Hopke, P.K., Rattigan, O.V., Xia, X., Chalupa, D.C., Utell, M.J., 2011a. Characterization of residential wood combustion particles using the two-wavelength aethalometer. Environ. Sci. Technol. 45, 7387–7393. http://dx.doi.org/10.1021/es2013984.

Wang, Y., Hopke, P.K., Rattigan, O.V., Zhu, Y., 2011b. Characterization of ambient black carbon and wood burning particles in two urban areas. J. Environ. Monit. 13, 1919–1926. http://dx.doi.org/10.1039/C1EM10117J.

World Health Organization, 2015. Residential Heating with Wood and Coal: Health Impacts and Policy Options in Europe and North America, vol. 58.